RNA & DISEASE 2022; 9: e1206. doi: 10.14800/rd.1206; © 2020 by Minyue Shou, *et al*.
http://www.smartscitech.com/index.php/RD

RESEARCH ARTICLE

MiR-1294, mediated by KLF4, negatively regulates cell proliferation and apoptosis by targeting MYH9 in Non-Small Cell Lung Cancer

Minyue Shou[1], Yongqian Shu[1,*]

Department of Oncology, The First Affiliated Hospital of Nanjing Medical University, Nanjing, Jiangsu 210029, China

[*] Correspondence: Yongqian Shu
E-mail: yongqian_shu@163.com
Received: May 15, 2022
Published online: June 1, 2022

Lung cancer, especially non-small cell lung cancer (NSCLC) is the most frequent cause of cancer-related mortality worldwide. MicroRNAs (miRNAs) represent a class of small non-coding RNA molecules. In recent years, many studies have confirmed that abnormal miRNAs expression in tumor can participate in many biological processes of NSCLC. However, whether miR-1294 is involved in the development of NSCLC remains unclear. In this study, miR-1294 was inhibited in NSCLC cell lines, and its expression was associated with tumor size and progression. MiR-1294 overexpression inhibited cell proliferation and cell cycle, conversely promoted cell apoptosis and senescence, and miR-1294 binding to MYH9 3'-UTR mediated suppression of it. Besides, three bioinformatics software were searched, and KLF4 was predicted as an upstream regulator of miR-1294. This study is the first to illuminate that miR-1294, mediated by KLF4, by targeting MYH9 to regulate NSCLC cell proliferation and apoptosis, and is a potential biomarker and therapeutic target for NSCLC.

Keywords: NSCLC, miRNAs, miR-1294, MYH9, KLF4

To cite this article: Minyue Shou, *et al*. MiR-1294, mediated by KLF4, negatively regulates cell proliferation and apoptosis by targeting MYH9 in Non-Small Cell Lung Cancer. RNA Dis 2022; 9: e1206. doi: 10.14800/rd.1206.

Abbreviations: CCK-8, Cell counting kit-8; ChIP, Chromatin Immunoprecipitation; DAB, diaminobenzidine; DIG, digoxin; EdU, 5-ethynyl-2'-deoxyuridine; EGFR, epidermal factor receptor; EMT, epithelial-mesenchymal transition; FBS, fetal bovine serum; IHC, immunohistochemistry; GAPDH, glyceraldehyde-3-phosphate dehydrogenase; GEO, Group on Earth Observation; ISH, in situ hybridization; KLF4, Kruppel-like factor 4; miRNA, micro ribonucleic acid; miR-1294, microRNA-1294; mTOR, mammalian target of rapamycin; MUT, mutant; MYH9, non-muscle myosin heavy chain Ⅱ A; NSCLC, non-small cell lung cancer; PI3K, phosphatidylinositol 3-kinase; PPAR, peroxisome proliferators-activated receptors; PTEN, phosphatase and tensin homolog; qRT-PCR, quantitative reverse transcriptase-polymerase chain reaction; TCGA, The Cancer Genome Atlas; TKI, tyrosine kinase inhibitor; UTR, untranslated region; WT, wild-type.

Introduction

Lung cancer is the most frequent cause of cancer-related mortality worldwide, with nearly 2.2 million new cases and 1.8 million deaths each year [1]. 85% of lung cancer patients are pathologically classified as non-small cell lung cancer (NSCLC) [2]. With the development of medical conditions, more and more lung cancer patients get timely diagnosis and surgical treatment in the early stage. The first-line chemotherapy drugs such as cisplatin for NSCLC

patients, receptor-tyrosine kinase inhibitor (TKI) for EGFR mutation patients, and PD-1/PD-L1 antibody has been gradually applied in the clinical treatment of lung cancer patients, which increased the five-year survival rate of lung cancer patients. However, with the passage of time, many patients began to develop different degrees of drug resistance. Therefore, to clarify the pathogenesis and progress of NSCLC and to solve the recurrence and metastasis of NSCLC is still a big problem to be solved in the near future.

MicroRNAs (miRNAs) represent a class of small non-coding RNA molecules with the ability to regulate target gene expression in a post-transcriptional manner. Its length is about 21-25nt, which is relatively short. However, miRNA plays an important role in various biological processes. In recent years, many studies have confirmed that abnormal miRNA expression in tumor can participate in many biological processes of tumor, such as cell proliferation, apoptosis, angiogenesis, aging, epithelial-mesenchymal transition (EMT), and drug resistance. The combination of miRNA diagnostic markers developed for different tumors has gradually started to be used in clinical practice, but its application and promotion are still limited. With the gradual improvement of RNA delivery efficiency, the development of miRNA related drugs has entered the clinical trial stage. Recent studies have shown that miR-1294 inhibits the proliferation and enhances the chemosensitivity of glioma to temozolomide via the direct targeting of TPX2 [3]. In gastric cancer, miR-1294 can alleviates EMT by repressing FOXK1 [4]. In addition, the low expression of miR-1294 is also related to the poor prognosis and tumor progression of epithelial ovarian cancer [5]. Similar results were obtained in research on the effect of miR-1294 on the invasion and proliferation of clear cell renal cell carcinoma [6]. However, whether mir-1294 is involved in the development of NSCLC remains unclear.

Non-muscle myosin heavy chain IIA (myosin-9, MYH9) belongs to the myosin superfamily of actin-binding motor protein. Recent studies have shown that MYH9 is involved in the proliferation, apoptosis and metastasis of a variety of cancer cells. In epithelial ovarian cancer and NSCLC, the high expression of MYH9 is closely related to tumor size, low differentiation with a more malignant nature, and its expression is an indicator of a poorer survival probability. In addition, MYH9 can significantly promotes growth and metastasis via activation of PI3K/AKT signaling in colorectal cancer [7]. The PI3K/AKT signaling as a classical signal pathway, is widely studied. Its phosphorylation activation is closely involved in the proliferation and apoptosis of tumor cells.

There are complex regulatory relationships among various molecules in vivo. Transcription factors and mRNA, as well as the regulation between miRNA and mRNA, are widely studied. In recent years, a large number of studies have demonstrated that the dysregulation of miRNA expression is also regulated by upstream transcription factors. Using online databases such as Jaspar and Transmir, we can predict the regulatory relationship between transcription factors and miRNAs. The regulatory relationship was further verified by Chromatin Immunoprecipitation, (ChIP) and other molecular biological experiments.

In this study, the role of miR-1294 in the development of NSCLC was studied in vitro, and its molecular mechanism was elucidated. We hope to find new targets and diagnostic markers for the treatment of NSCLC through this study.

Materials and Methods

Human NSCLC specimens

Fifty NSCLC tissue samples and the corresponding adjacent noncancerous specimens from NSCLC cases treated in the First Affiliated Hospital of Nanjing Medical University from 2015 to 2016 were assessed. Exclusion criteria for sample collection were: preoperative administration, chemotherapy, or a history of other malignancies. These clinical samples were rigorously confirmed pathologically, and each tissue pair was immediately placed in liquid nitrogen after surgical resection from patients with NSCLC. This study had approval from the Ethics Committee of the First Affiliated Hospital of Nanjing Medical University. Patients have signed the relevant informed consent before the operation. We collected pathological report and related medical record information two weeks after the operation, and the relevant data were recorded.

Cell lines and culture

Five human lung carcinoma cell lines, including A549, H358, H1299, SPC-A1, PC-9, and the noncancerous human bronchial epithelial (BEAS-2B) cell line, all provided by ATCC (USA), were assessed in this study. SPC-A1 cells culture was performed in DMEM, and the others were performed in RPMI 1640 (Gibco, USA). Medium contained 10% fetal bovine serum (FBS), 100 U/ml penicillin and 100 mg/ml streptomycin (Gibco), in an incubator containing 5% CO2 at a temperature of 37°C. We took 2 ml to observe the sample in small dish to prevent contamination of medium.

In situ hybridization (ISH) staining

To determine miR-1294 level in human NSCLC tissues and adjacent tissues, the situ hybridization was involved in this study. Fresh tissue in liquid nitrogen was removed and placed immediately in the stationary solution, then was dehydrated by decreasing concentration of alcohol followed by wax embedding. All paraffin-embedded tissue sections were dewaxed and rehydrated, and were digested using Proteinase K (20μg/ml) at 37℃. After digestion, tissue sections were washed three times with PBS and incubated with digoxin (DIG) probe for miR-1294 oligopolymer (Servicebio, China) overnight at 37℃. Anti-DIG-labeled peroxidase was subsequently added for 40 minutes. All sections were stained by 3,3-diaminobenzidine (DAB) solution and positive results were exhibited as brownish yellow. The nuclei were counterstained with hematoxylin.

RNA extraction and quantitative reverse transcription PCR

Total RNA was extracted from the tissues and cells by TRIzol reagent (EpiZemy, China) according to the manufacturer's instructions. Real-time fluorescence quantitative polymerase chain reaction (qRT-PCR) were used to detect the relative expression of miR-1294 in cancer tissues, paracancerous tissues, bronchial epithelial cells (BEAS-2B) and NSCLC cells. PrimeScript™II Reverse Transcriptase (RiboBio, China) was involved to generate cDNA, and qRT-PCR was analyzed by SYBR Green Master Mix II (Takara, Japan). The results of CT values were derived using storage devices and converted by $2^{-\Delta\Delta Ct}$ method to quantify the relative expression levels of miR-1294. Each sample was run in triplicate.

Cell transduction

The control lentivirus, miR-1294 interference and overexpression virus were transfected with Polybrene (5μg/ml) respectively (GenePharma, China). Then we exchanged cell fluid. The cells transfected with the virus were able to survive when they were screened with purinomycin because they inserted the purinomycin resistance gene, while the remaining cells were killed as the concentration of purinomycin increased. Then, stably transduced cells were selected using puromycin (2μg/ml). For MYH9 plasmids, si-GRB2, or corresponding controls were transfected with Lipofectamine 3000 (Invitrogene, USA) based on the protocols.

Cell proliferation assay

Cell counting kit-8 (CCK-8) and EdU experiment were used to detect the effect of miR-1294 on cell proliferation. Transfected NSCLC cells were incubated into the plates (96 well) and then were cultured with CCK-8 solution (Dojindo, Japan). 60μl of reagents (10μl of CCK8 solution and 50μl of serum-free medium) were added to each well to calculate the total volume of reagents needed for measurement, and the CCK8 and serum-free medium were mixed at 1:5 configuration. Incubator was placed for 30 minutes, and the enzyme labeling instrument determined the absorbance value at 450 nm per hole by using a spectrophotometer (ThermoFisher, Rockford, USA).

EdU assay was carried out using EdU Kit (Ribobio, China) based on the instructions. Dilute in the medium at 1:1000 and add the mixed liquid to the 24-well plate one by one. Transfected cells were incubated with EdU (50μM) for 2h. Through using a fluorescence microscope the positive cells were screened by Apollo staining. Then we counted the total number of cells in the field of vision, and the number of cells in the proliferative state using Image J. The result was showed as the percentage of EdU-positive in total DAPI-positive cells.

Flow cytometric assessment

DNA Staining solution (1ml) and Permeabilization solution (10μl) were added to the EP tube and conserved without light at room temperature for 30 minutes. We used a stored procedure in a flow cytometry machine to detect cell cycle (Beyotime, China). Logarithmic growth cells were cultured overnight, and then digested by 0.25% trypsin (excluding EDTA). We used the method of AnnexinV-PI double staining and detected by Annexin-V/FITC apoptosis detection kit (Beyotime, Shanghai, China).

Luciferase reporter assay

Three bioinformatics websites (Targetscan, Mirtarbase and Starbase) were used to predict the downstream target gene of miR-1294. Venn diagram was used to intersect the results of the three websites. The luciferase reporter gene assays were used to prove whether MYH9 was the direct target gene of miR-1294. The 3'-UTR sequence or the mutant sequence of MYH9 was inserted into pmir-GLO-promoter vector (Promega, USA). MYH9-WT cells and MYH9-MUT cells were transfected with miR-1294 mimic or negative control. After transfection, cells were transfected with the co-transfection of corresponding plasmids and internal parameters (0.05μg Sea kidney luciferase expression plasmid) by Lipofectamine 2000 reagent (Invitrogene, USA). The activity of luciferase values was evaluated with GloMax detector (Promega, USA).

Western blotting

Total protein of cells was extracted from the cells with cell lysis buffer, containing 150 mM NaCl, 2 μg/ml

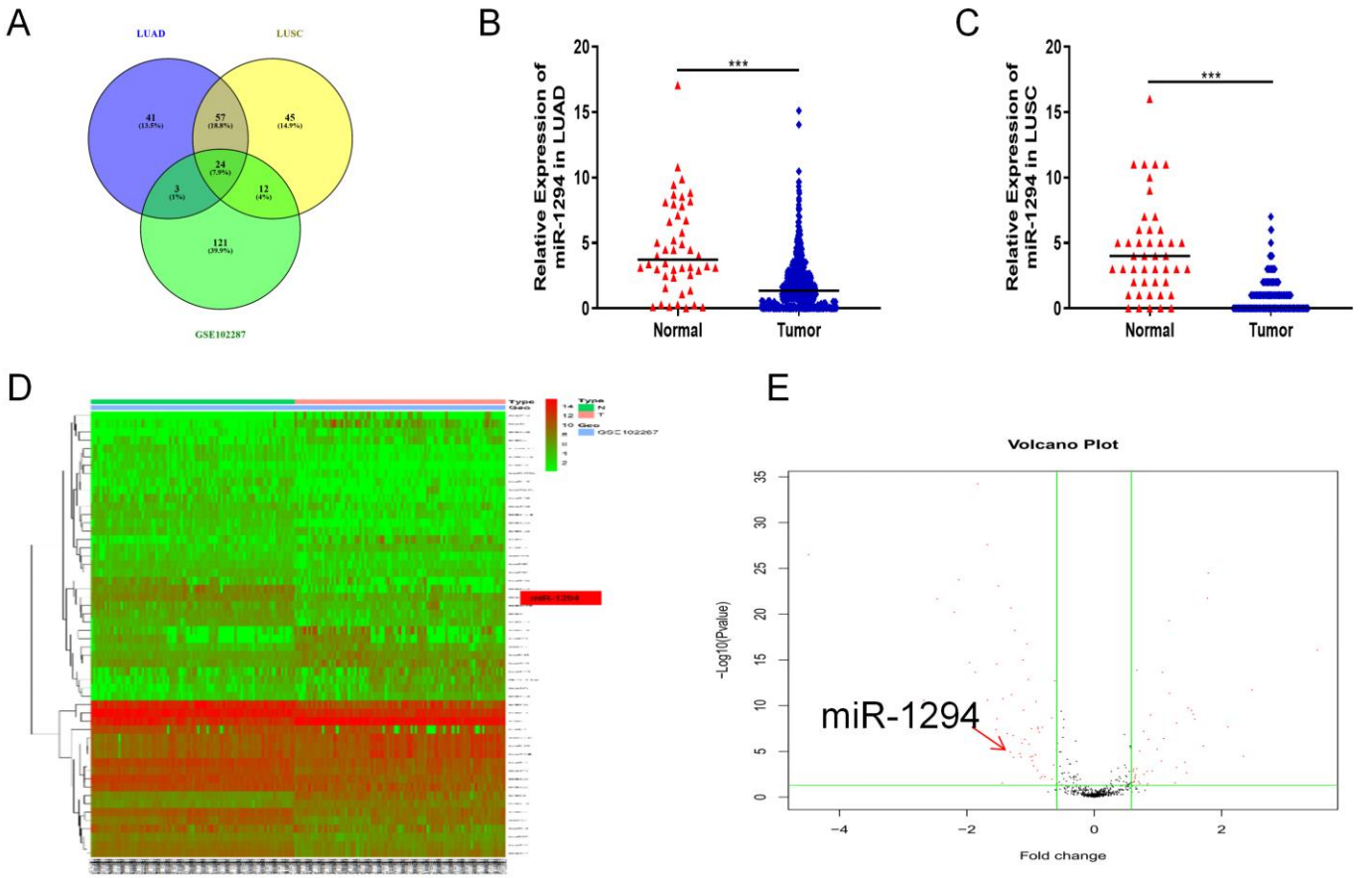

Fig. 1. MiR-1294 expressed relatively low in TCGA-LUAD、TCGA-LUCC and GEO chips (GSE102287). (A) TCGA-LUAD, TCGA-LUSC, and GSE102287 were downloaded to search for miRNAs with different expression and to conduct the intersection. Select the appropriate miRNA candidates from the intersection of the three chips. (B) MiR-1294 expression in the TCGA-LUAD. (C) MiR-1294 expression in the TCGA-LUAD. (D) Heat map by GSE102287 chips. (E) Volcanic blot by GSE102287 chips. Data are expressed as mean ± SD. ***indicated P＜0.001.

Aprotinin, 1% NP-40, 0.1% SDS, 1.5 mM EDTA, 2 μg/ml Leupeptin, and 1 mM PMSF. Concentration of protein samples was measured using the BCA kit (Beyotime, China). The protein lysates were separated by 10% SDS-polyacrylamide gel and then transferred to PVDF membrane (Roche, USA). After being transferred into 5% skim milk (PBST preparation) and incubated at room temperature for 1~2 hours, the PVDF membrane was incubated overnight at 4℃ with the primary antibodies of MYH9 (ThermoFisher). The secondary antibodies (ThermoFisher) corresponding to the primary antibodies were inquired and detected by an enhanced chemiluminescence (ECL) system (ThermoFisher).

Immunohistochemistry (IHC)

All the samples were fixed with formalin and embedded in paraffin, and then paraffin sections dewaxed to water. Sections were soaked in citrate antigen repair buffer (pH6.0) and the repair was completed by microwave heating. The tissue sections were sealed with serum BSA (Servicebio, China) and incubated at room temperature for 30 minutes. The tissue sections were incubated with primary antibodies for MYH9 (ThermoFisher) and Ki-67 that has been diluted with PBS proportionally overnight at 4℃. Then the sections were incubated with the secondary HRP antibodies of the corresponding species (ThermoFisher) at room temperature for 50 minutes and stained with DAB solution (Servicebio, China). The nuclei were counterstained with hematoxylin for 3 minutes. A positive optical microscope (Nikon, Japan) was used to evaluate the images.

Chromatin Immunoprecipitation (ChIP)

It was operated through ChIP kit (Millipore, USA). The

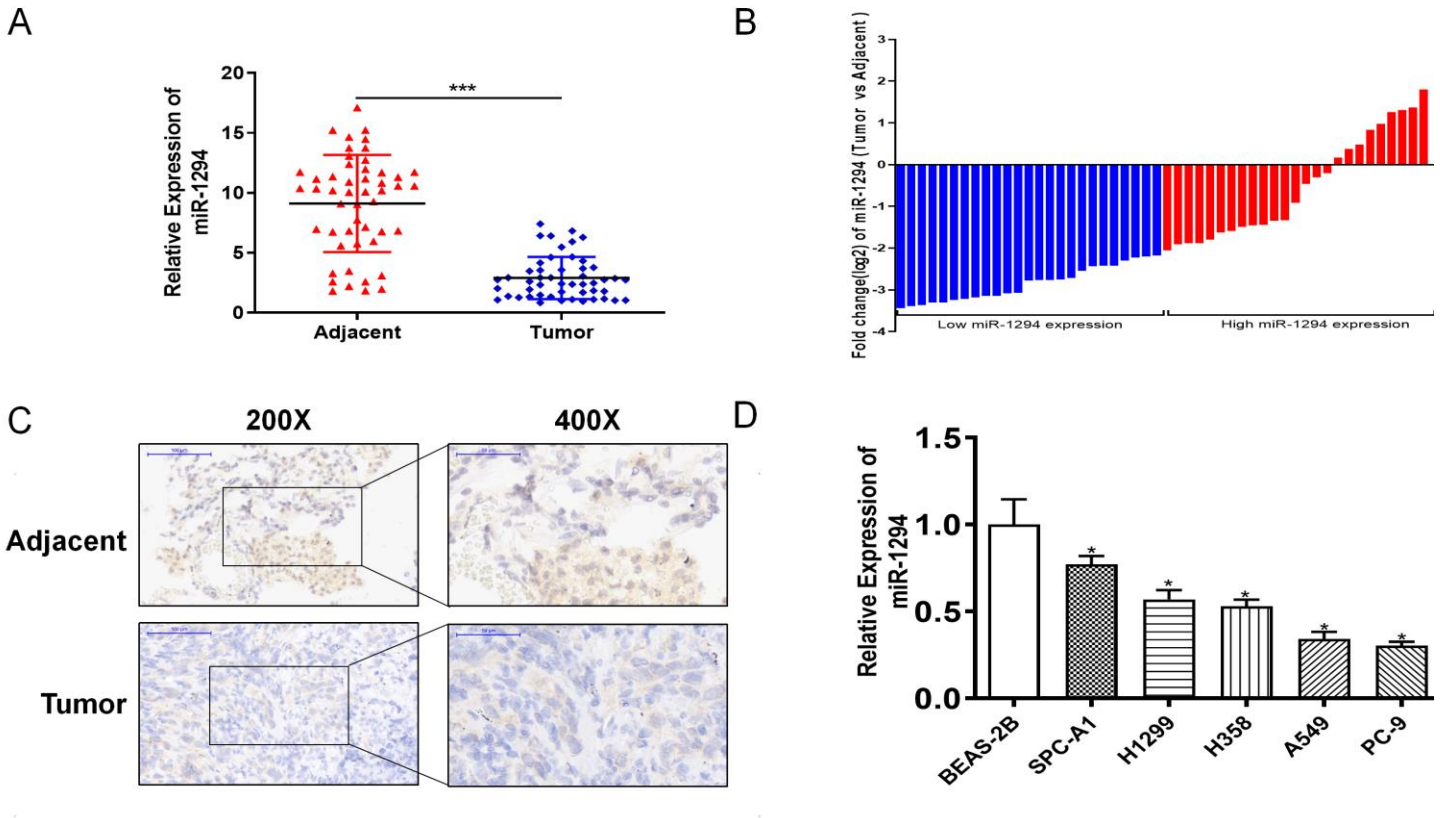

Fig. 2. MiR-1294 is relatively low expressed in human NSCLC tissues and cell lines. (A) Detection of miR-1294 expression levels by qRT-PCR in NSCLC tissues and paired adjacent lung tissues (n=50). (B) The fold change (log2 change) of miR-1294 levels between NSCLC patients tumor and paired adjacent tissues was assessed, then separated into low miR-1294 expression group or high miR-1294 expression group according to the median level of miR-1294 (n = 50). (C) ISH staining against miR-1294 was conducted in NSCLC patients tumor and paired adjacent tissues. (D) MiR-1294 expression in different NSCLC cells (SPCA-1, H1299, H358, A549, PC-9) and normal lung epithelial cell (BEAS-2B) were detected using qRT-PCR. Data are expressed as mean ± SD. *indicated P＜0.05, ***indicated P＜0.001.

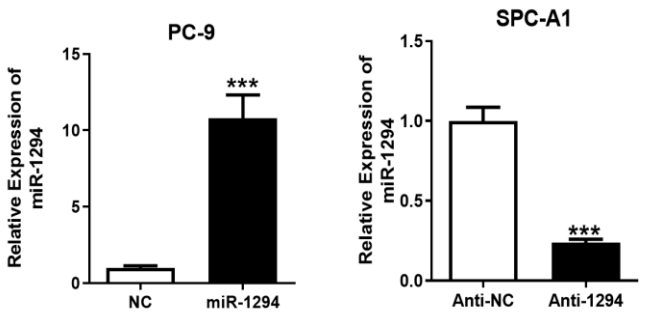

Fig. 3. Detection of miR-1294 expression in PC-9, SPC-A1, and control cells by qRT-PCR after lentivirus transfection. Data are expressed as mean ± SD. ***indicated P＜0.001.

cells were fixed with formaldehyde (1%) and cracked after collected. DNA was degraded into small fragments of chromatin of 200–800 bp by sonication. ChIP antibodies that added to the target protein were incubated at 4℃ overnight. Then we added Protein A Beads and incubated at 4℃ for 60 minutes, thus precipitated the antibody-protein-DNA complex. After eluting nonspecific binding, then separating and purificatiing ChIP DNA, we verified whether DNA fragment contained the target fragment using qRT-PCR. GAPDH was an internal reference.

Results

miR-1294 was decreased both in NSCLC tissues and cell lines

We first searched three data sets (TCGA-LUAD, TCGA-LUSC, GEO chip (GSE102287)) for miRNAs with different expression and to screen the intersection through wayne graph. There were 24 miRNAs included in the intersection of the three datasets (miR-21, miR-210, miR-96, miR-708, miR-183, miR-141, miR-200a, miR-301a, miR-135b, miR-130b, miR-130b, miR-454, miR-93, miR-345, miR-503, miR-301b, miR-31, miR-200b, miR-224, miR-891a, miR-1294, hsa-let-7c, miR-143, miR-144, miR-30a) (Fig. 1A). Of them, the role of miR-1294 in NSCLC

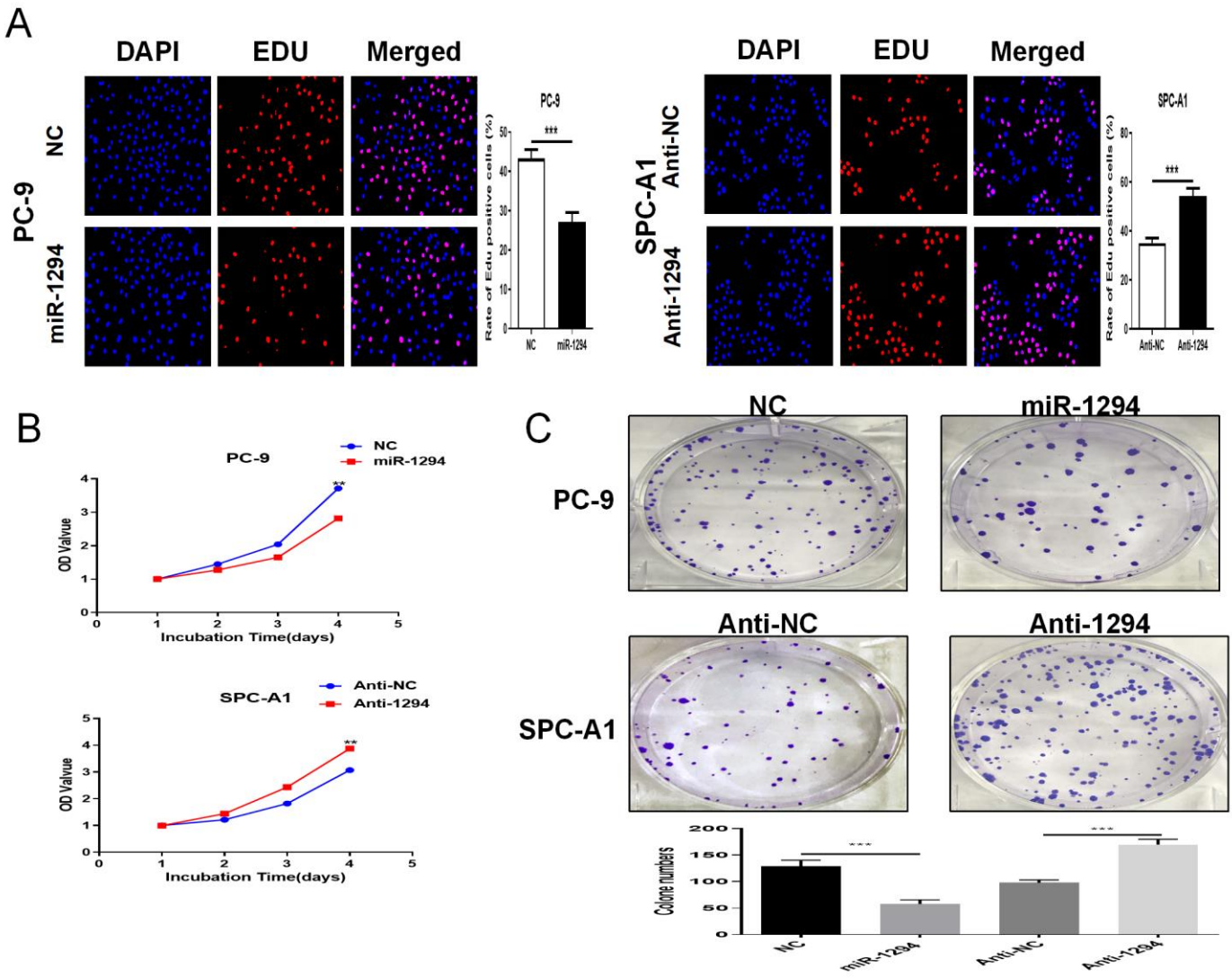

Fig. 4. MiR-1294 inhibites the proliferation of NSCLC cells. (A) Effects of miR-1294 on proliferation of PC-9 and SPC-A1 cells were determined by cell counting kit-8 (CCK-8) experiments. (B) Effects of miR-1294 on proliferation of PC-9 and SPC-A1 cells were determined by EdU experiments. (C) Effects of miR-1294 on proliferation of PC-9 and SPC-A1 cells were determined by clone formation experiments. Data are expressed as mean ± SD. **indicated P＜0.01, ***indicated P＜0.001.

was never reported. We continued to analyze the expression of miR-1294 in the above three datasets, and used GSE102287 to generate Volcano Plot and Heat Map. The results showed that miR-1294 was relatively low expressed in NSCLC tissues (Fig. 1B,C,D,E).

To clarify the relative expression levels of miR-1294 in NSCLC tissues, we detected previously collected NSCLC tissues and matched adjacent tissues from NSCLC patients for qRT-PCR detection. As presented in Table 1, miR-1294 was significantly related to tumor size (P<0.05), but no difference was observed among gender, age, smoking behavior, and pathology. Compared with adjacent noncancerous samples and bronchial epithelial cells, miR-1294 is relatively down-regulated in NSCLC tissue and cell lines (Fig. 2A,B). Then we randomly selected 15 pairs of specimens for in situ hybridization (DAB staining). The staining of NSCLC tissues was lighter compared with adjacent tissues (brownish yellow when DAB positive) (Fig. 2C), indicating that miR-1294 was low expressed in NSCLC. Furthermore, we uncovered that among the NSCLC cell lines, PC-9 cells had the lowest miR-1294 expression, whereas SPC-A1 cells had the highest one (Fig. 2D).

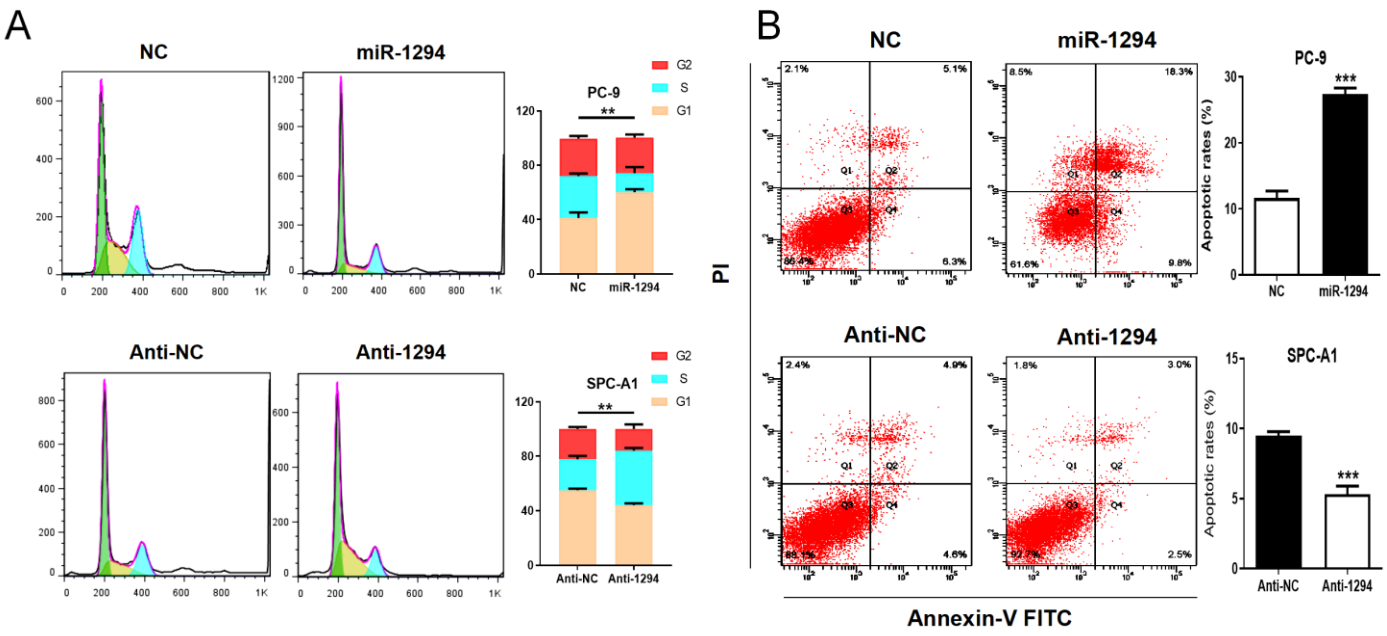

Fig. 5. MiR-1294 inhibits the division of PC-9 and SPC-A1 cells and promotes their apoptosis. (A) Determine the effect of miR-1294 on cell cycle by flow cytometry. (B) Determine the effect of miR-1294 on apoptosis by flow cytometry. Data are expressed as mean ± SD. **indicated P＜0.01, ***indicated P＜0.001.

Table 1. Relationship between miR-1294 expression level and clinical features of NSCLC patients.

Clinicopathological features	MiR-1294 expression level		*P* value
	high	low	
Gender			0.569
Male	13	15	
Female	12	10	
Age			0.560
≥60	8	11	
<60	17	14	
Smoking behavior			0.778
Yes	13	11	
No	12	14	
Pathology			0.762
Squamous cell carcinoma	7	9	
Adenocarcinoma	18	16	
Size of tumor			0.033*
T1-T2	21	13	
T3-T4	4	12	

Biological function of miR-1294 in NSCLC

We selected miR-1294-transfected PC-9 cells and anti-1294-transfected SPC-A1 cells to detect the relative expression of the miR-1294 by qRT-PCR respectively. From the results, we observed miR-1294 was upregulated in the miR-1294-transfected PC-9 cells compared with the control groups, and downregulated in the anti-1294-transfected SPC-A1 cells compared with the control groups (Fig. 3). Both CCK-8 (Fig. 4A) and EdU (Fig. 4B) assays showed that overexpression of miR-1294 could inhibit the proliferation and division of lung cancer cells. miR-1294 expression was revealed to be downregulated in PC-9 cells, exerting a promoting effect on cell proliferation, while high expression of miR-1294 in SPC-A1 cells exerted an inhibition effect. We performed clone formation experiment to verify that miR-1294 promote the apoptosis and inhibit the progression of lung cancer cells (Fig. 4C).

Division exuberantly is a sign of tumor cells. As an experimental result of flow cytometry, in the analysis of cell cycle, percentage of PC-9 cells overexpressed miR-1294 significantly increased in the G0/G1 stage; while the SPC-A1 cells transfected to interfere with the virus had the opposite results (Fig. 5A). The result in the apoptosis analysis was similar. Overexpression of miR-1294 could increase the proportion of apoptotic cells compared with control group, while knocking down miR-1294 could reduce the proportion of apoptotic cells (Fig. 5B).

MYH9 overexpressed in NSCLC was the direct target gene of miR-1294

A large number of studies have shown that miRNA, downstream target genes together with the signal pathways regulated by target genes constitute a complex regulatory

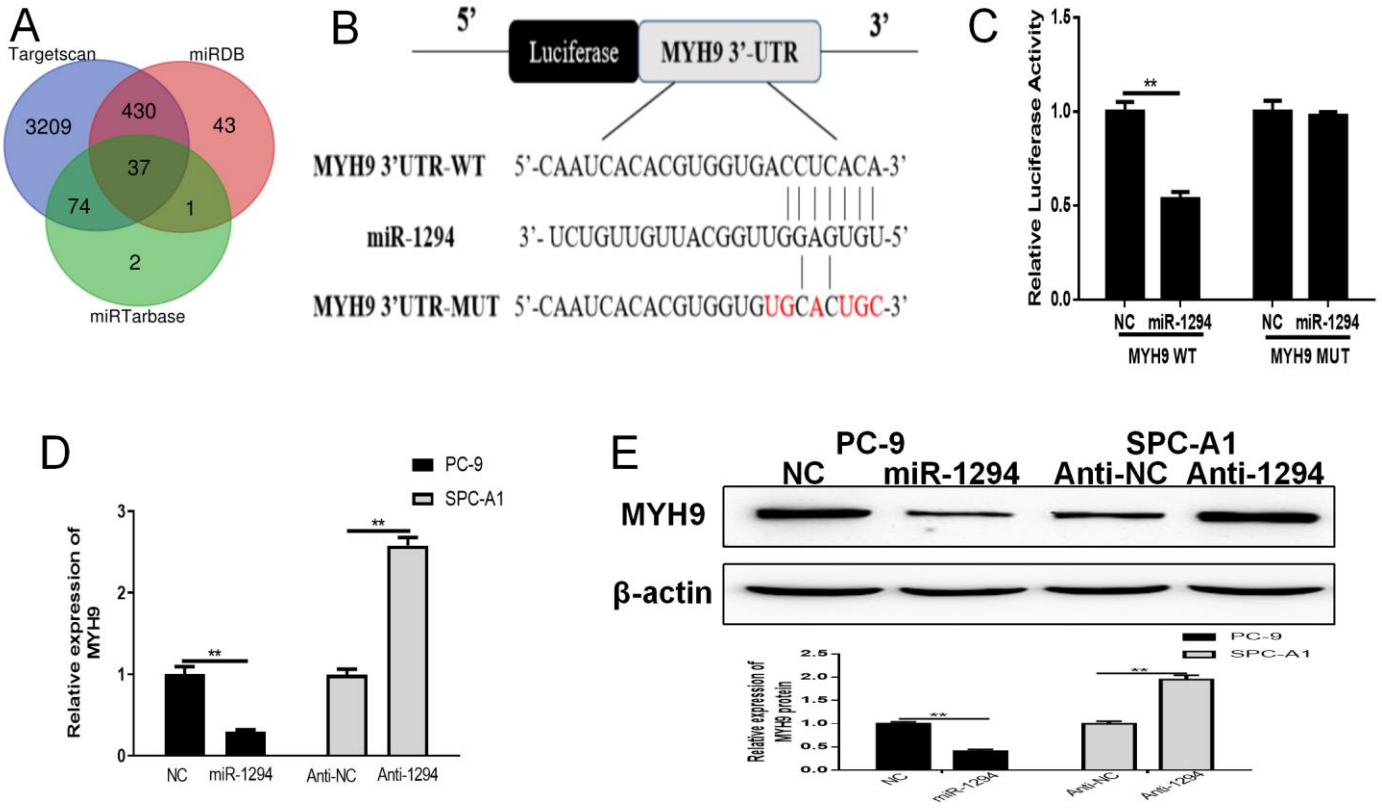

Fig.6. MiR-1294 regulates MYH9 by interacting with the 3'-UTR region of MYH9. (A) Three different prediction websites (TargetScan, miRDB, and miRTarbase) were used to predict candidate gene targets and used the Venn diagram to intersect the results. (B) Luciferase reporter was used to investigate whether miR-1294 regulates MYH9 by bonding to the 3'-UTR region of MYH9. (C) Luciferase reporter was carried out in cells co-transducted with miR-1294-mimics and MYH9-WT or MYH9-MUT compared with control groups. (D) MYH9 expression at mRNA levels after knocking down or over-expressing miR-1294 by qRT-PCR. (E) Protein expression levels of MYH9 in transducted PC-9 and SPC-A1 cells using Western blot. Data are expressed as mean ± SD. **indicated $P<0.01$.

network. We predicted candidate gene targets by interesting outputs from three distinct prediction algorithms (TargetScan, miRDB, miRTarbase) (Fig. 6A). From the resultant list of 37 genes, we focused on the factors that are upregulated in NSCLC. The prediction revealed that miR-1294 had binding sites with the 3'-UTR of MYH9. We constructed MYH9 wild-type (WT) and mutant (MUT) reporter gene plasmids and performed luciferase reporter gene experiments (Fig. 6B). Luciferase activity was significantly decreased compared with control group after co-transfection of miR-1294 mimics and MYH9-WT reporter gene plasmids; while co-transfected miR-1294minics and MYH9-MUT reporter gene plasmids, luciferase activity did not change significantly (Fig. 6C). In addition, we detected the expression of MYH9 at the level of mRNA and protein by qRT-PCR and Western blotting and explored that overexpression of miR-1294 significantly decreased the expression of MYH9 compared with the control group in PC-9 cells, while knockdown of miR-1294 elevated the expression level of MYH9 in SPC-A1 (Fig. 6D,E).

MYH9 is overexpressed in NSCLC tissues and cells

We performed qRT-PCR on fifty NSCLC tissue samples and the corresponding adjacent noncancerous specimens, and the results showed that the expression level of MYH9 was higher in NSCLC tissues than which in adjacent noncancerous tissues (Fig. 7A). After retrieving the pathology and related information of fifty NSCLC patients (Table 2), it was found that MYH9 expression level also had a significant correlation with tumor size ($p<0.05$), while there was no significant correlation with gender, age, smoking behavior, and pathology type. Correlation analysis showed a negative correlation between miR-1294 and MYH9 expression in NSCLC tissues ($R^2=0.2988$, $p<0.01$) (Fig. 7B), suggesting that 3'-UTR of MYH9 was the direct target gene of miR-1294. The results of immunohistochemical staining of 15 randomly paired tissue samples illustrate this result as well (Fig. 7C). We continued to test MYH9 expression levels in BEAS-2B cell

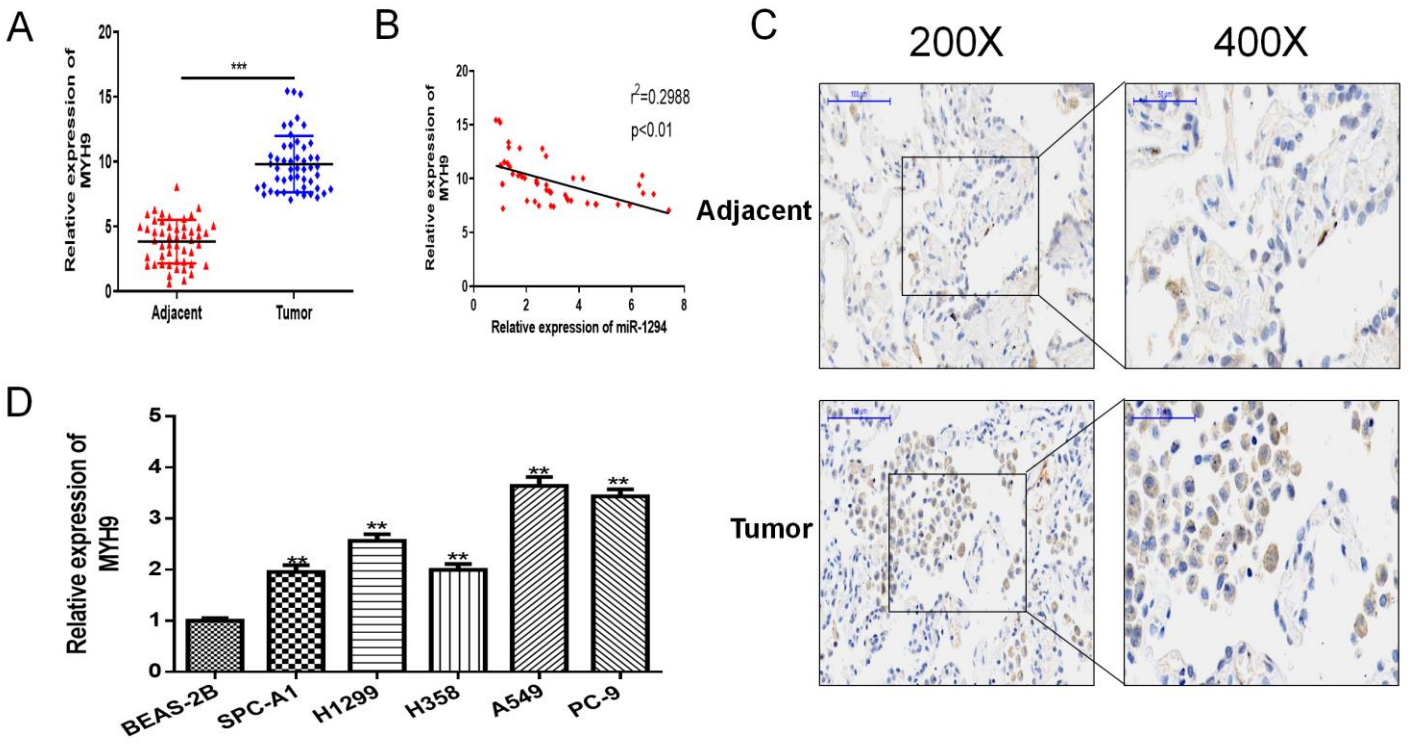

Fig. 7. MYH9 is relatively overexpressed in human NSCLC tissues and cell lines. (A) The expression of MYH9 at mRNA levels was assessed in patients tumor and paired adjacent tissues (n = 50). (B) The results of correlation analysis demonstrated negative correlation between miR-1294 and MYH9 expression in NSCLC tissues (r^2=0.2988). (C) IHC staining against MYH9 was performed in NSCLC patients tumor and adjacent tissues (n=15). (D) Expression levels of MYH9 in different NSCLC cell lines (SPCA-1, H1299, H358, A549, PC-9) and normal lung epithelial cell (BEAS-2B) were detected using qRT-PCR. Data are expressed as mean ± SD. **indicated P＜0.01, ***indicated P＜0.001.

lines and NSCLC cell lines (SPC-A1, H1299, H358, A549, PC-9). In our verification, the expression of MYH9 in all five NSCLC cell lines was markedly higher than that in BEAS-2B (Fig. 7D). All of these results suggest that MYH9 is downstream target gene regulated by miR-1294.

Table 2. Relationship between MYH9 expression level and clinical features of NSCLC patients.

Clinicopathological features	MYH9 expression level		*P* value
	high	low	
Gender			0.569
Male	12	16	
Female	13	9	
Age			0.560
≥60	12	7	
<60	13	18	
Smoking behavior			0.778
Yes	10	14	
No	15	11	
Pathology			0.762
Squamous cell carcinoma	6	10	
Adenocarcinoma	18	16	
Size of tumor			0.033*
T1-T2	12	22	
T3-T4	13	3	

miR-1294 targeted MYH9 to regulate biological function in NSCLC

We transfected plasmid overexpressed MYH9 into PC-9 cells that overexpressed miR-1294, while transfected si-MYH9 plasmid into SPC-A1 cells that knocked out miR-1294. Then we detected the expression of MYH9 at mRNA and protein levels by qRT-PCR and Western blotting (Fig. 8A,B). The results showed that co-transfection of MYH9 plasmid could restore MYH9 expression level compared with overexpression miR-1294 alone, while the expression level of MYH9 decreased after transfection of si-MYH9 sequence compared with individual knocking out miR-1294. It suggests that there is reverse regulation of miR-1294 to its downstream gene MYH9. To further investigate whether miR-1294 targeting MYH9 to regulate the biological function in NSCLC, we performed CCK-8 cell proliferation experiments (Fig. 9A), EdU cell proliferation experiments (Fig. 9B), and clonal formation experiments (Fig. 9C). The results showed that cotransfection with MYH9 overexpression plasmid reversed the inhibitory effect of miR-1294 on cell proliferation compared with miR-1294 overexpression alone, while the proliferation level of lung cancer cells was reduced after cotransfection

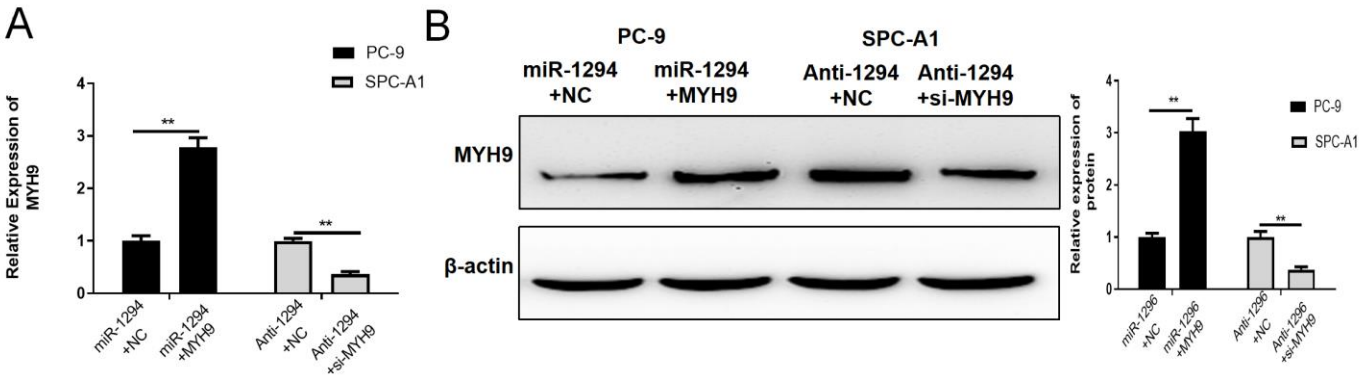

Fig. 8. MiR-1294 negatively regulates the expression of MYH9. (A) mRNA expression levels of MYH9 in co-transduced PC-9 and SPC-A1 were assessed using qRT-PCR. (B) Protein expression levels of MYH9 in co-transduced PC-9 and SPC-A1 were assessed using Western blot. Data are expressed as mean ± SD. **indicated P＜0.01.

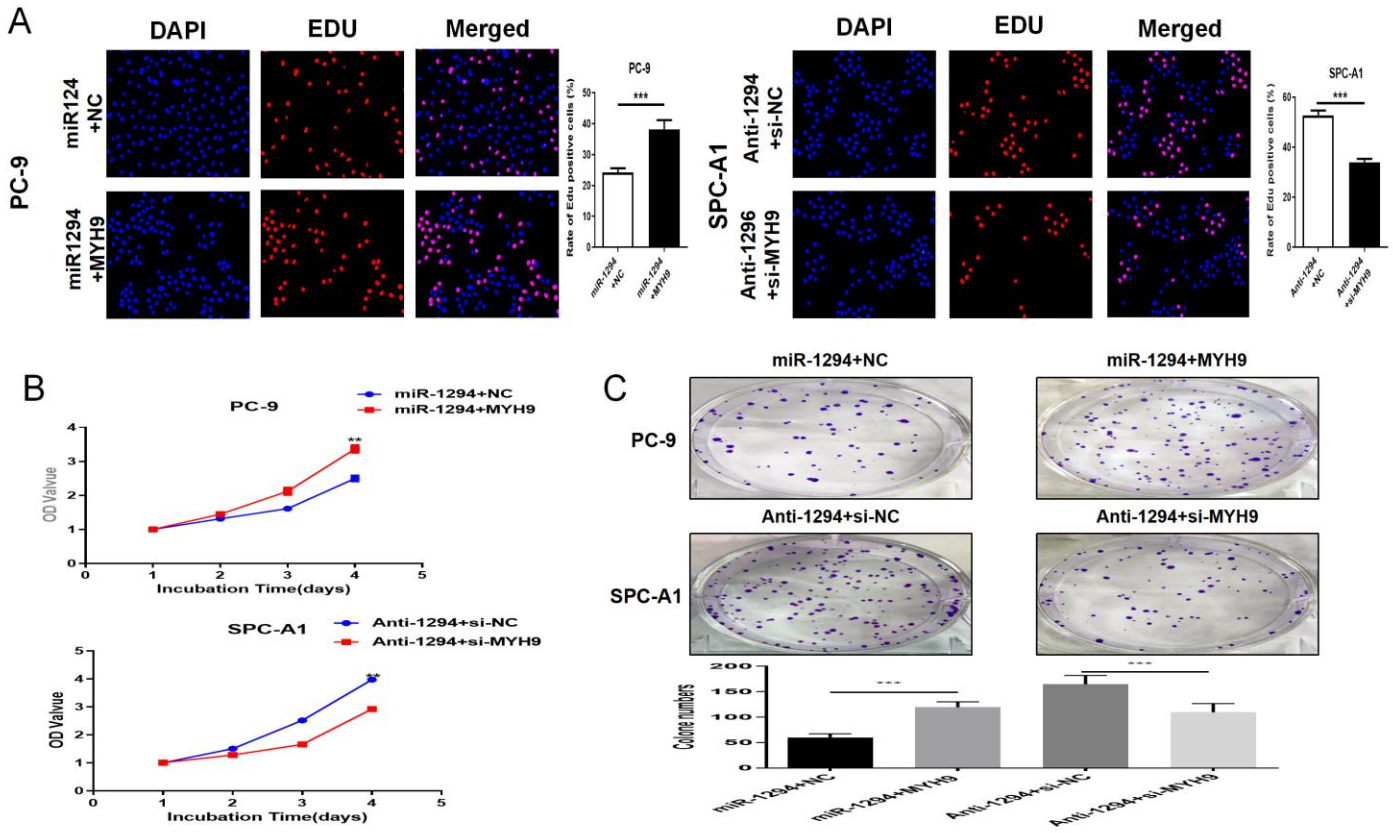

Fig. 9. MiR-1294 targeted MYH9 to reduce the proliferative capacity of PC-9 and SPC-A1 cells. (A, B, C) CCK-8, EdU and clone formation experiments were used to detect the effects of miR-1294 and MYH9 on proliferation of PC-9 and SPC-A1 cells. Data are expressed as mean ± SD. **indicated P＜0.01, ***indicated P＜0.001.

with MYH9 small interfering sequence compared with miR-1294 knockdown alone.

Flow cytometric detection of cell cycle (Fig.10A) and apoptosis (Fig.10B) in the treated and control groups revealed that the percentage of G0/G1 phase cells was significantly lower after cotransfection with MYH9 overexpression plasmid compared to miR-1294 alone, and the percentage of G0/G1 phase cells was increased after cotransfection with MYH9 small interfering sequence compared to miR-1294 knockdown alone. These findings

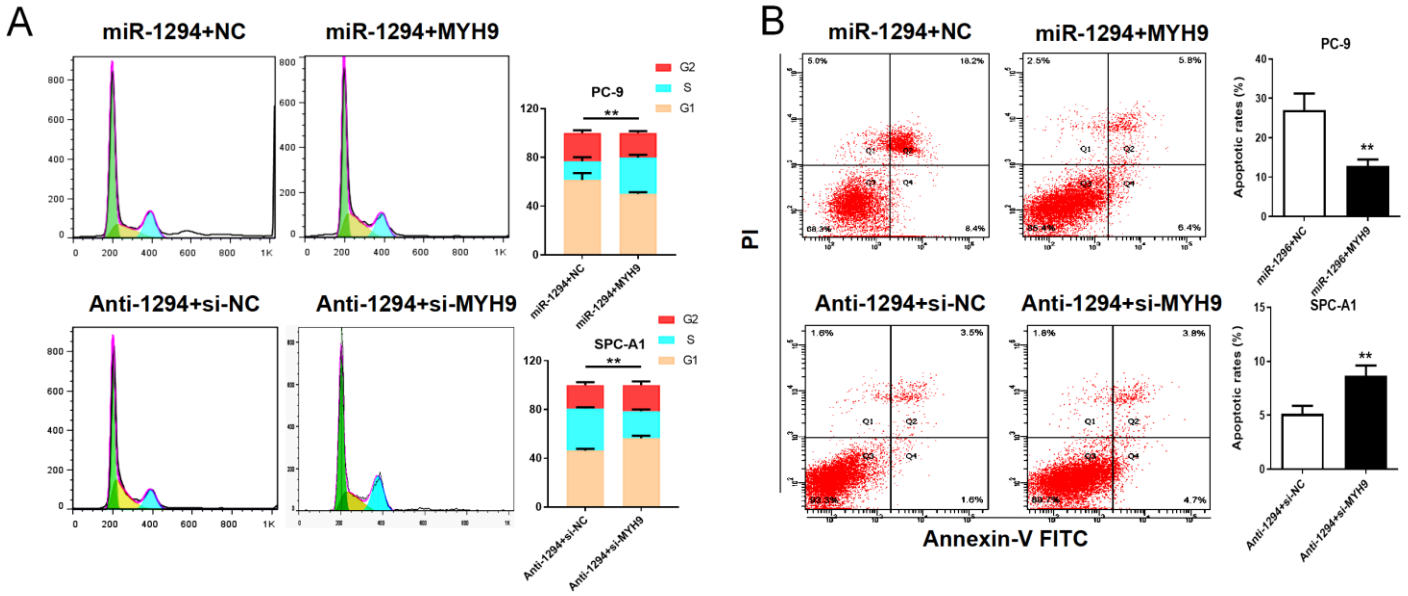

Fig. 10. MiR-1294 could delay the process and promote cell apoptosis of PC-9 and SPC-A1 cell cycle by negatively regulating MYH9. (A) Determine the effect of miR-1294 and MYH9 on cell cycle by flow cytometry. (B) Determine the effect of miR-1294 and MYH9 on apoptosis by flow cytometry. Data are expressed as mean ± SD. **indicated P＜0.01.

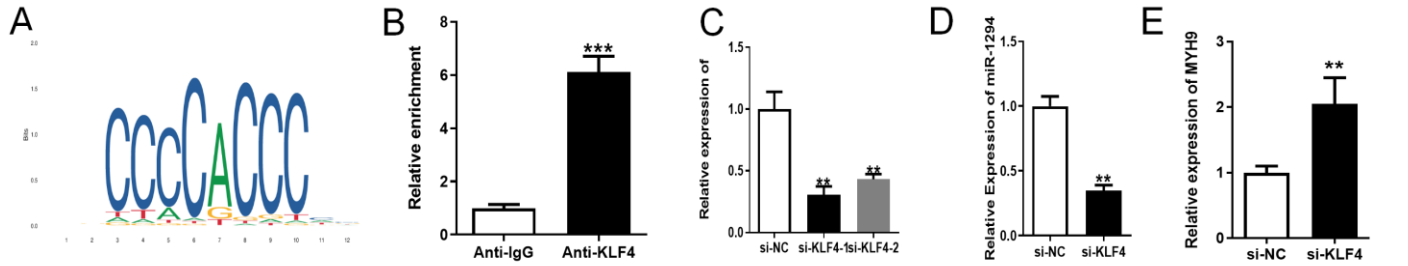

Fig. 11. KLF4 was an upstream regulator of miR-1294. (A) Jaspar was used to predict the transcription factors that regulate the expression of miR-1294. (B) Whether KLF4 is involved in the regulation of miR-1294 expression was verfied by ChIP sample analysis. (C) The efficiency of si-KLF4 knocking out KLF-4 was verified by qRT-PCR. (D) Changes of miR-1294 expression levels after knocking out KLF4 by qRT-PCR. (E) Changes of MTH9 expression levels after knocking out KLF4 by qRT-PCR. Data are expressed as mean ± SD. **indicated P＜0.01, ***indicated P＜0.001.

demonstrated that miR-1294 inhibited the cell division cycle and promoted cell apoptosis by targeting MYH9 and overexpression of MYH9 could reverse these effects induced by miR-1294.

KLF4 was an upstream regulator of miR-1294

To identify upstream regulators that may be responsible for miR-1294 overexpression in NSCLC, based on Jaspar database, we found that the putative score of KLF4 binding to miR-1294 was the highest that might be potential upstream regulator of miR-1294 (Fig. 11A). We carried out ChIP experiment to deposit the DNA fragments bound to KLF4, then we verified whether KLF4 bound to the promoter region of the miR-1294 by qRT-PCR (Fig. 11B). We further used si-KLF4 sequence to conduct rescue experiments, the expression of miR-1294 decreased and the expression of MYH9 increased (Fig. 11C,D,E). These results confirmed that KLF4 can participate in the regulation of miR-1294 expression. KLF4 is upregulated in lung cancer tissues, and acts as a multifunctional transcription factor.

To investigate the effects of KLF4 on cell proliferation and apoptosis, we conducted EdU cell proliferation experiments (Fig. 12A) and used flow cytometric analysis to detect apoptosis levels (Fig. 12B). Compared with the control group, the cell proliferation level increased and the proportion of apoptotic cells decreased after transfection of si-KLF4. To further investigate whether KLF4 are involved in miR-1294 regulation of the biological function of lung

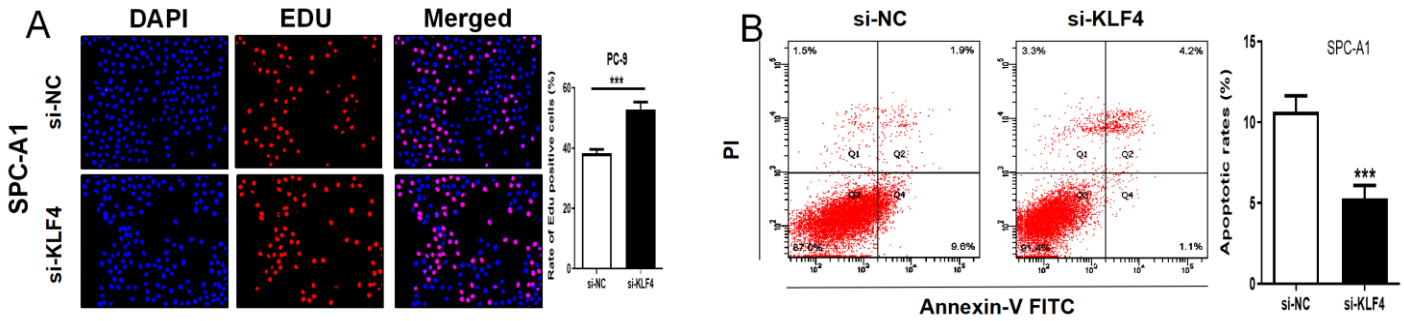

Fig. 12. KLF4 inhibits the proliferation of NSCLC cells and promotes apoptosis. (A) EdU experiments were used to detect the effect of KLF4 on cell proliferation capacity. (B) Flow cytometry was used to detect the effect of KLF4 on apoptosis. Data are expressed as mean ± SD. ***indicated P ＜0.001.

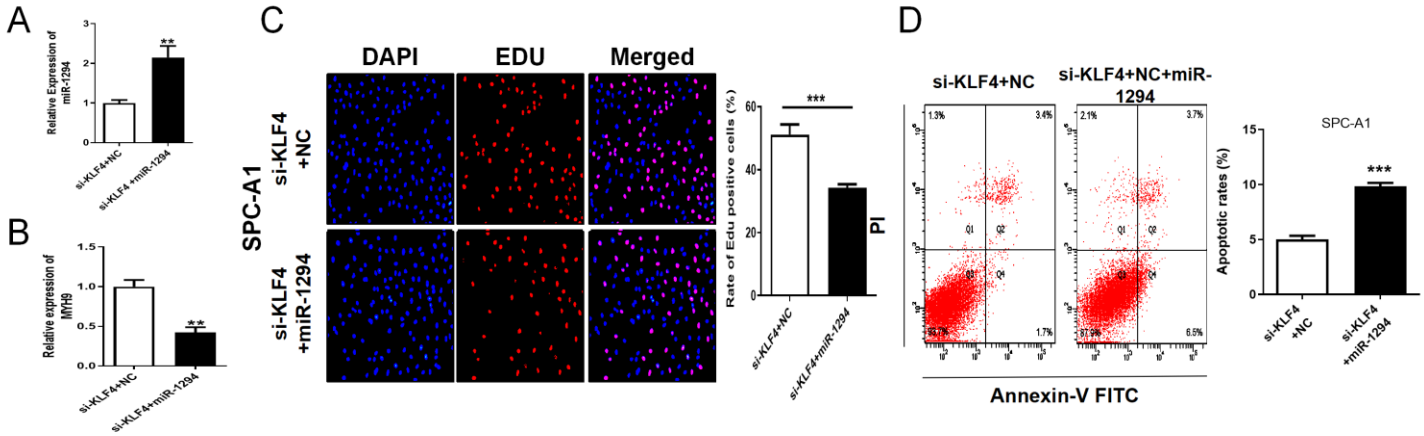

Fig. 13. KLF4 positively regulates miR-1294 to inhibit the proliferation of NSCLC cells and promote their apoptosis. (A,B) MiR-1294 and MYH9 expression after co-transfecting miR-1294 and si-KLF4 were detected by qRT-PCR. (C) EdU experiments to detect the effect of co-transfection of si-KLF4 with miR-1294 on the proliferative capacity of SPC-A1 cells. (D) Flow cytometry to detect the effect of si-KLF4 with miR-1294 on apoptosis of SPC-A1 cells. Data are expressed as mean ± SD. **indicated P＜0.01, ***indicated P＜0.001.

cancer cells, we co-transfected si-KLF4 into SPC-A1 cells which had co-transfected miR-1294 overexpressed viruses. Compared with knockdown of KLF4 alone, overexpression of miR-1294 was followed by a decrease in MYH9 expression (Fig. 13A,B). Subsequent EdU cell proliferation experiments (Fig. 13C) and apoptosis experiments (Fig. 13D) showed that miR-1294 overexpression could partially rescue the effects of si-KLF4 on cell proliferation and apoptosis in SPC-A1 cell lines. The total results indicated that KLF4 contributed to the inhibition of cell proliferation and promotion of cell apoptosis by modulating miR-1294 transcription.

Discussion

In our study, we acquired relatively reliable target genes of miR-1294 through Targetscan, miRDB and miRTarbase three major gene prediction software by intersection processing. The predictive results showed that miR-1294 had a good targeting relationship with MYH9. Then we confirmed that compared with expression of MYH9 in adjacent normal tissues, it can be seen that the expression of MYH9 in NSCLC tissues showed a clear upward trend, while the expression of miR-1294 showed the completely converse situation. By double luciferase reporter gene detection test and the correlation analysis of the expression of MYH9 and miR-1294 level in NSCLC tissues, we clarified that there was a negative correlation between the expression of miR-1294 and MYH9. The results also proved that miR-1294 can inhibit the translation of target genes and then regulate their protein levels by western blotting. On one hand, it shows that miR-1294 is likely to play a role in antitumous effect by targeting regulatory MYH9 in the human body. On another hand, the research

of miR-1294/MYH9 is of great significance to reveal the occurrence and development of NSCLC and provide a new therapeutic target. To further define our results, we conducted rescue experiment which confirmed that MYH9 recombination or knockdown partially rescued the miR-1294 mediated effect. In addition, we further predicted KLF4 as the upstream regulator of miR-1294 through the database. Our multiple experimental results suggested that KLF4 is involved in miR-1294 regulation of NSCLC. Overall, the total results indicated that KLF4 contributed to the inhibition of cell proliferation and promotion of cell apoptosis by modulating miR-1294 transcription. Our research illuminated that miR-1294, mediated by KLF4, by targeting MYH9 to regulate NSCLC cell proliferation and apoptosis.

It is a common feature that miRNAs abnormally expressed during the development and progression of the tumor. They target oncogenes or tumor suppressor genes, and their expression spectrum is closely related to the embryonic origin of the tumor. Therefore, its expression has tissue specificity, which can serve as a useful tumor diagnosis marker. According to the different influence in tumor cells, miRNAs can be divided into carcinogenic and suppressor miRNAs [8]. Carcinogenic miRNAs promote the growth of cancer cells by down-regulating the expression of tumor suppressor gene. Conversely, tumor suppressor miRNAs combine with oncogene at the transcriptional level and inhibit its expression, so as to inhibit the growth of tumor cells. The mechanism of miRNAs regulating gene expression is mainly combined with complementary loci of target mRNAs, which impede the translation of mRNAs or lead to their degradation. MiRNAs usually target 3'-UTR of mRNAs, but there are also studies suggest that miRNAs can be combined with 5'-UTR of some mRNAs to regulate the expression of homologous protein. One miRNA can regulate hundreds of target genes expression under this mechanism. Similarly, one target gene may be regulated by hundreds of miRNAs. In addition, miRNAs adjust their target genes, going with changes in the expression of downstream genes which are regulated by the target genes. MiRNAs, their target genes and other downstream genes constitute complicated network system together. It is important to maintain the balance of each node in this system, then normal cell cycle can be guaranteed. If the balance is broken, it may lead to the development of various diseases including cancer. Therefore, it is particularly necessary to understand how miRNAs function and affect the relevant signaling pathways in cells.

In recent years, a series of research prove that miR-1294 is a novel tumor suppressor miRNA discovered in glioma [3], gastric cancer [4], epithelial ovarian cancer [5], and renal cell carcinoma [6]. However, the relationship between miR-1294 and NSCLC is remained to be explored. In previous studies, we detected the expression of miR-1294 in NSCLC tissues was significantly decreased compared with matched adjacent normal tissues, which was the same as NSCLC cells. The expression level of miR-1294 in SPC-A1, H1299, H358, A549, and PC-9 NSCLC cell lines was lower than that of normal cell lines. The above results suggest that miR-1294 may play a role in tumor inhibition in the development of NSCLC and work by regulating downstream target genes.

MYH9 belongs to the myosin superfamily of actin-binding motor proteins, encoding non-muscle myosin heavy chain IIA [9]. There are 15 classes of myosin superfamily. Myosin II is a type of conventional biceps myosin which can form two-stage filaments that are directly involved in regulating cytoplasmic division, cell movement, and cell morphology in non-muscle cells. Because of MYH9 contributes to cell polarization, connectivity, separation, and transfer [10,11], it plays an important role in tumor cell migration, invasion and metastasis [12,13]. Ken Katono *et al.* have shown that the high expression of MYH9 in lung cancer tissues is related to intratumoral vascular invasion and lymph node metastasis, and can be used as an independent risk factor for the prognosis of NSCLC, which indicated that MYH9 has certain value in tumor invasion and metastasis and prognosis judgment. The expression of MYH9 is closely related to tumor size, low differentiation and poor prognosis in epithelial ovarian cancer and NSCLC. It had been shown that MYH9 significantly promotes colorectal cancer by regulating PI3K/AKT signaling pathways [7]. PI3K/AKT, as a widely studied classical signaling pathway, its phosphorylation activation is closely involved in proliferation and apoptosis of tumor cells [14]. We were also able to further examine the expression levels of total protein and phosphorylated protein of AKT and its key molecule mTOR in the signaling pathway by Western blotting to clarify the role of MYH9 in PI3K/AKT signaling pathway.

As mentioned above, there are complex regulatory relationships among miRNAs and mRNAs. However, mechanisms to control miRNA expression under normal and pathological conditions have not been fully investigated. In recent years, it proves that transcription factors are responsible for dysregulated expression of miRNAs in cancers [15,16]. For example, Dharap A *et al.* have shown that the activation of PPARγ can regulate the expression of miR-145 and miR-329 [17], while Zhong Y *et al.* have found that the key transcription factor AP-1 and downstream miRNAs together constitute the PTEN regulatory network in the model of liver ischemia-

reperfusion injury [18]. It is of great significant for elucidating the role of miRNAs in tumors to investigate the regulatory role of transcription factors on miRNA expression [19]. Through the database, we found that KLF4 is the upstream transcription factor of miR-1294. KLF4 is a specific biological zinc finger protein transcription factor with binding sites, which belongs to the KLF protein family and is mainly expressed in digestive and epithelial cells. KLF4 mainly contains three domains: DNA binding domain, transcriptional regulatory domain and nuclear localization sequence. As a transcription factor, KLF4 can regulate downstream genes and thus participate in many biological processes including cell proliferation, apoptosis, and so on. In many malignant diseases, such as esophageal squamous cell carcinoma [20], gastric cancer [21], lung cancer [22], carcinoma of urinary bladder [23], prostatic carcinoma [24], and colorectal cancer [25], the expression of KLF4 is down-regulate, while it is inverse in mammary cancer [26] and oral squamous cell carcinoma [27]. Other studies have found that KLF4 can participate in the occurrence and progression of NSCLC by silencing a series of miRNAs, such as miR-3120 [28], miR-3182 [29], miR-1915 [30], and our study demonstrates the role of KLF4 in the development of NSCLC through the regulation of miR-1294. Glibenclamide targeting SUR1 upregulates the expression of the oncogene KLF4 to inhibit NSCLC [31], and KLF4 is closely associated with A549 cisplatin resistance in NSCLC [32]. As a consequence, KLF4 could be a potential therapeutic target in NSCLC.

In summary, there is a KLF4-miR1294-MYH9 axis existing in NSCLC. The results of our study have identified: (1) the relationship between NSCLC and level of miR-1294 and MYH9; (2) miR-1294 can regulate the expression of MYH9, and then inhibit the biological process of NSCLC; (3) there is a positive correlation between miR-1294 and KLF4 regulated signaling pathway. MiR-1294 may become new therapeutic targets and diagnostic markers for non-small cell lung cancer in the future. As mentioned above, the research on MYH9-regulated signaling pathways was deficient in our study, and although the possibility of MYH9 targeting AKT signaling pathway was proposed, further validation was required. In addition, our study was limited to cell lines, and the findings need further but in vivo validation.

Ethics Approval

This case series was approved by the institutional ethics board of The First Affiliated Hospital of Nanjing Medical University, and consent was obtained from patients.

Conflicting Interests

The authors declare that they have no conflict of interests.

Acknowledgements

This work was supported by National Natural Science Foundation of China (grant no. 82172889).

References

1. Sung H, Ferlay J, Siegel RL, et al. Global Cancer Statistics 2020: GLOBOCAN Estimates of Incidence and Mortality Worldwide for 36 Cancers in 185 Countries. *CA: a cancer journal for clinicians.* 2021;71(3):209-249.
2. Warth A, Endris V, Penzel R, Weichert W. [Molecular pathology of lung cancer. State of the art 2014]. *Der Pathologe.* 2014;35(6):565-573.
3. Chen H, Liu L, Li X, Shi Y, Liu N. MicroRNA-1294 inhibits the proliferation and enhances the chemosensitivity of glioma to temozolomide via the direct targeting of TPX2. *Am J Cancer Res.* 2018;8(2):291-301.
4. Shi YX, Ye BL, Hu BR, Ruan XJ. Expression of miR-1294 is downregulated and predicts a poor prognosis in gastric cancer. *Eur Rev Med Pharmacol Sci.* 2018;22(17):5525-5530.
5. Guo TY, Xu HY, Chen WJ, Wu MX, Dai X. Downregulation of miR-1294 associates with prognosis and tumor progression in epithelial ovarian cancer. *Eur Rev Med Pharmacol Sci.* 2018;22(22):7646-7652.
6. Pan W, Pang LJ, Cai HL, Wu Y, Zhang W, Fang JC. MiR-1294 acts as a tumor suppressor in clear cell renal cell carcinoma through targeting HOXA6. *Eur Rev Med Pharmacol Sci.* 2019;23(9):3719-3725.
7. Wang B, Qi X, Liu J, et al. MYH9 Promotes Growth and Metastasis via Activation of MAPK/AKT Signaling in Colorectal Cancer. *Journal of Cancer.* 2019;10(4):874-884.
8. Ye G, Fu G, Cui S, et al. MicroRNA 376c enhances ovarian cancer cell survival by targeting activin receptor-like kinase 7: implications for chemoresistance. *J Cell Sci.* 2011;124(Pt 3):359-368.
9. Palandri F, Zoli M, Polverelli N, et al. MYH9-related thrombocytopenia and intracranial bleedings: a complex clinical/surgical management and review of the literature. *Br J Haematol.* 2015;170(5):729-731.
10. Vicente-Manzanares M, Ma X, Adelstein RS, Horwitz AR. Non-muscle myosin II takes centre stage in cell adhesion and migration. *Nat Rev Mol Cell Biol.* 2009;10(11):778-790.
11. Conti MA, Adelstein RS. Nonmuscle myosin II moves in new directions. *J Cell Sci.* 2008;121(Pt 1):11-18.
12. Derycke L, Stove C, Vercoutter-Edouart AS, et al. The role of non-muscle myosin IIA in aggregation and invasion of human MCF-7 breast cancer cells. *Int J Dev Biol.* 2011;55(7-9):835-840.
13. Betapudi V, Licate LS, Egelhoff TT. Distinct roles of nonmuscle myosin II isoforms in the regulation of MDA-MB-231 breast cancer cell spreading and migration. *Cancer Res.* 2006;66(9):4725-4733.
14. Katono K, Sato Y, Jiang SX, et al. Prognostic significance of MYH9 expression in resected non-small cell lung cancer. *PLoS One.* 2015;10(3):e0121460.

15. Jiang L, Yu X, Ma X, et al. Identification of transcription factor-miRNA-lncRNA feed-forward loops in breast cancer subtypes. *Comput Biol Chem.* 2019;78:1-7.
16. Xia Y, Wei K, Yang FM, et al. miR-1260b, mediated by YY1, activates KIT signaling by targeting SOCS6 to regulate cell proliferation and apoptosis in NSCLC. *Cell Death Dis.* 2019;10(2):112.
17. Dharap A, Pokrzywa C, Murali S, Kaimal B, Vemuganti R. Mutual induction of transcription factor PPARγ and microRNAs miR-145 and miR-329. *J Neurochem.* 2015;135(1):139-146.
18. Zhong Y, Zhu Y, Dong J, et al. Identification of Key Transcription Factors AP-1 and AP-1-Dependent miRNAs Forming a Co-Regulatory Network Controlling PTEN in Liver Ischemia/Reperfusion Injury. *Biomed Res Int.* 2019; 2019: 8962682.
19. Lin Y, Duan Z, Xu F, Zhang J, Shulgina MV, Li F. Construction and analysis of the transcription factor-microRNA co-regulatory network response to Mycobacterium tuberculosis: a view from the blood. *Am J Transl Res.* 2017;9(4):1962-1976.
20. Luo A, Kong J, Hu G, et al. Discovery of Ca2+-relevant and differentiation-associated genes downregulated in esophageal squamous cell carcinoma using cDNA microarray. *Oncogene.* 2004;23(6):1291-1299.
21. Kim B, Bang S, Lee S, et al. Expression profiling and subtype-specific expression of stomach cancer. *Cancer Res.* 2003; 63(23):8248-8255.
22. Bianchi F, Hu J, Pelosi G, et al. Lung cancers detected by screening with spiral computed tomography have a malignant phenotype when analyzed by cDNA microarray. *Clin Cancer Res.* 2004;10(18 Pt 1):6023-6028.
23. Ohnishi S, Ohnami S, Laub F, et al. Downregulation and growth inhibitory effect of epithelial-type Krüppel-like transcription factor KLF4, but not KLF5, in bladder cancer. *Biochem Biophys Res Commun.* 2003;308(2):251-256.
24. Luo J, Dunn T, Ewing C, et al. Gene expression signature of benign prostatic hyperplasia revealed by cDNA microarray analysis. *Prostate.* 2002;51(3):189-200.
25. Xu J, Lü B, Xu F, et al. Dynamic down-regulation of Krüppel-like factor 4 in colorectal adenoma-carcinoma sequence. *J Cancer Res Clin Oncol.* 2008;134(8):891-898.
26. Foster KW, Frost AR, McKie-Bell P, et al. Increase of GKLF messenger RNA and protein expression during progression of breast cancer. *Cancer Res.* 2000;60(22):6488-6495.
27. Huang CC, Liu Z, Li X, et al. KLF4 and PCNA identify stages of tumor initiation in a conditional model of cutaneous squamous epithelial neoplasia. *Cancer Biol Ther.* 2005;4(12):1401-1408.
28. Xu H, Wen Q. miR-3120-5p acts as a diagnostic biomarker in non-small cell lung cancer and promotes cancer cell proliferation and invasion by targeting KLF4. *Molecular medicine reports.* 2018;18(5):4621-4628.
29. Zheng G, Huang J, Chen W, You P, Ding Y, Tu P. circUBAP2 exacerbates malignant capabilities of NSCLC by targeting KLF4 through miR-3182 modulation. *Aging.* 2021;13(8):11083-11095.
30. Pan H, Pan Z, Guo F, et al. MicroRNA-1915-3p inhibits cell migration and invasion by targeting SET in non-small-cell lung cancer. *BMC cancer.* 2021;21(1):1218.
31. Xu K, Sun G, Li M, et al. Glibenclamide Targets Sulfonylurea Receptor 1 to Inhibit p70S6K Activity and Upregulate KLF4 Expression to Suppress Non-Small Cell Lung Carcinoma. *Molecular cancer therapeutics.* 2019;18(11):2085-2096.
32. Liu M, Li X, Peng KZ, et al. Subcellular localization of Klf4 in non-small cell lung cancer and its clinical significance. *Biomedicine & pharmacotherapy.* 2018;99:480-485.

Supporting Information

Table S1. PCR primers used for plasmid construction.

ICP27(2)-CACC-F	CACCATGGCTACCGACATTG
ICP27(2)-717STOP-R	CTACGCCTTTCGCTCCGGGA
ICP27(2)-718-CACC-F	CACCCCCTCTGCCGACACCATC
ICP27(2)-STOP-R	CTAAAATAGGGAGTTGC
ICP27-169STOP	CCGGCGCGTCTCCAGATAGGCCCACAAC
ICP27-169STOP(-)	GTTGTGGGCCTATCTGGAGACGCGCCGG
ICP27-153STOP	GGGGTCGATACGGCTAGGGCGGCGCCGACTC
ICP27-153STOP(-)	GAGTCGGCGCCGCCCTAGCCGTATCGACCCC
ICP27-138STOP	CACCGCATCCCTGAGGCGGGCGG
ICP27-138STOP(-)	CCGCCCGCCTCAGGGATGCGGTG
ICP27-d1-152	GATGACAAGAAGCTTGGATCCCCCGGCGGCGCCGACTCCAC
ICP27-d1-152(-)	GTGGAGTCGGCGCCGCCGGGGGATCCAAGCTTCTTGTCATC
ICP27-d1-168	GATGACAAGAAGCTTGGATCCAACGCCCACAACCAAGGGGG
ICP27-d1-168(-)	CCCCCTTGGTTGTGGGCGTTGGATCCAAGCTTCTTGTCATC
ICP27-d1-109	GATGACAAGAAGCTTGGATCCACCAGGCGGTCGGCTTCCCCC
ICP27-d1-109(-)	GGGGGAAGCCGACCGCCTGGTGGATCCAAGCTTCTTGTCATC
ICP27-450STOP	TGTCGGAGATCGACTACACGTAGAATTCCCGGGTCGACTC
ICP27-450STOP(-)	GAGTCGACCCGGGAATTCTACGTGTAGTCGATCTCCGACA
ICP27-368STOP	GGTGCAAGATGTGCATTTAGCACAATCTGCCGCTCC
ICP27-368STOP(-)	GGAGCGGCAGATTGTGCTAAATGCACATCTTGCACC
ICP27-282STOP	CAAGACCCCTTTGGCTAGATGCCGTTTCCCGC
ICP27-282STOP(-)	GCGGGAAACGGCATCTAGCCAAAGGGGTCTTG

Table S2. PCR primers used for EMSA probe preparation.

T7-UL18-335F	TAATACGACTCACTATAGGGATCCCGTCAGCCTCGTC
UL18-434R	GTTGGGAGCGGGACCGGAAACC
T7-UL27-2480F	TAATACGACTCACTATAGGGAGGAAGGCGCGGAGG
UL27-2579R	TCCGTGCGCTCCATGGCCGAC
T7-UL29-2490F	TAATACGACTCACTATAGGGCAAGCCCCCGGGGTCGAAC
UL29-2589R	CTCTATGTCCTCGCGCGACAAGAG
T7-US10-629F	TAATACGACTCACTATAGGGTTCATACCCAATGGCTTCGGGCC
US10-728R	TGGACGCAGGGCGCAGCCG
T7-UL39-1976F	TAATACGACTCACTATAGGGCGTGCGTGTACCTGGAACC
UL39-2075R	AAGATGTTGTCGCAGCGCTGGGCC
T7-UL21-290F	TAATACGACTCACTATAGGGACCCGAACGTGAGCTCCGAGC
UL21-389R	GGGCTGGTTCGCAGCGAGGTG
T7-RL2-2171F	TAATACGACTCACTATAGGGCCTCTTCCTCCGCCGCCCC
RL2-2270R	CGGTCGCCCGAGTCCGAGTCC
T7-US4-1798F	TAATACGACTCACTATAGGGATCCGCCCCACGCTCCCGCC
US4-1897R	TGGGGCCCGAGGGCATGTCCTTAG
T7-UL42-516F	TAATACGACTCACTATAGGGCGACCCCGACGTCCAG
UL42-615R	GCCGAGCTCGAACGTGGTGGGTTTG
T7-UL26-1559F	TAATACGACTCACTATAGGGACACGGAGACCCCCGCCCAAC
UL26-1658R	ACCGCCCCGGATAGAGGAGGC
T7-UL27-2379F	TAATACGACTCACTATAGGGCTACGTCCTGCAACTGCAACG
UL27-2678R	TGGAGCGGAGAGTACCTGGC
T7- UL42-417F	TAATACGACTCACTATAGGGCATATGGACGACCGCGTCCG
UL42-716R	AGAATCTGGACCTGGGCGCTG
T7-US12-1F	TAATACGACTCACTATAGGGATGTCTTGGGCCCTGAAAACGAC
US12-261R	TCAAGGGGCCAGCACGCGATCC